Earth and Planetary Science Letters 377–378 (2013) 239–247

Contents lists available at SciVerse ScienceDirect

Earth and Planetary Science Letters

www.elsevier.com/locate/epsl

Controls on the seasonal deformation of slow-moving landslides

Alexander L. Handwerger [a,*], Joshua J. Roering [a], David A. Schmidt [b]

[a] Department of Geological Sciences, University of Oregon, 1272 University of Oregon, Eugene, OR 97403-1272, USA
[b] Department of Earth and Space Sciences, University of Washington, 4000 15th Ave NE, Seattle, WA 98195-1310, USA

ARTICLE INFO

Article history:
Received 30 January 2013
Received in revised form 28 June 2013
Accepted 29 June 2013
Available online 25 July 2013
Editor: P. Shearer

Keywords:
landslides
hydrology
precipitation
InSAR
lidar
pore-water pressure diffusion

ABSTRACT

Precipitation drives seasonal velocity changes in slow-moving landslides by increasing pore-water pressure and reducing the effective normal stress along basal shear zones. This pressure change is often modeled as a pore-water pressure wave that diffuses through the landslide body, such that the minimum time required for landslides to respond to rainfall should vary as the square of landslide depth (which often approximates the saturated thickness) and inversely with hydraulic diffusivity. Here, we assess this model with new observations from the landslide-prone Eel River catchment, Northern California. Using satellite radar interferometry (InSAR) time series, precipitation data, and high-resolution topographic data from airborne lidar, we quantify the seasonal dynamics of 10 slow-moving landslides, which share the same lithologic, tectonic, and Mediterranean climate conditions. These slope failures have areas ranging from 0.16 to 3.1 km^2, depths that vary from 8 to 40 m, and average downslope velocities of 0.2 to 1.2 m/yr. Each slide exhibits well-defined seasonal velocity changes with a periodicity of ~1 yr and responds (i.e., accelerates) within 40 days following the onset of rainfall. Despite a five-fold variation in landslide depth, we do not detect systematic differences in response time within the resolution of our observations. Our results could imply that: 1) slides in our study area are sensitive to subtle hydrologic perturbations, 2) the 'effective' diffusivity governing slide behavior is much higher than field-derived values because pore pressure transmission and slide dynamics are facilitated by preferential flow paths, particularly cracks related to deformation and seasonal shrink-swell cycles, or 3) a simple one-dimensional linear diffusion model may fail to capture the three-dimensional time-dependent hydrologic changes inherent in an evolving mechanical–hydrologic system, such as a slow-moving landslide.

1. Introduction

Slow-moving landslides cause significant erosion, regulate hillslope angles and topographic relief, and are a principle geologic hazard that damages infrastructure. These slope failures are driven by hydrologic forcing and typically respond to precipitation (i.e., accelerate) over seasonal time scales through increased pore-water pressure and reduced effective normal stress along basal shear zones (Terzaghi, 1950). Quantifying the interaction between precipitation and landslide mobility is essential for characterizing the role of landslides in landscape evolution and hazard mitigation. Slow-moving landslides are found in diverse climatic and geological settings, and when examined in detail, do not exhibit straightforward relationships between precipitation, topographic slope, and velocity; yet, they frequently exhibit a seasonal pattern of acceleration and deceleration (Iverson and Major, 1987; Coe et al., 2003; Hilley et al., 2004; Calabro et al., 2010; Scheingross et al., 2013). These slope failures accelerate within days to months after the onset of rainfall and decelerate into the dry season, with some coming to a halt. Periods of acceleration are correlated with increasing pore-water pressures caused by infiltration of precipitation, whereas periods of deceleration are typically correlated with decreasing pore-water pressures caused by drainage, and, potentially from dilation of the shear zone material (Iverson and Major, 1987; Coe et al., 2003; Iverson, 2005; Schulz et al., 2009). There is ample evidence from laboratory experiments (Iverson et al., 2000; Moore and Iverson, 2002) and numerical models (Iverson, 2005) to support the occurrence of shear zone dilation, but field evidence is limited (Schulz et al., 2009). Mechanical–hydrologic feedbacks facilitate seasonal sliding that can persist for hundreds or even thousands of years (Bovis and Jones, 1992; Mackey et al., 2009; Rutter and Green, 2011; Coe, 2012), although slow-moving landslides can sometimes fail catastrophically without warning (Petley et al., 2002).

Numerical models and field-based measurements suggest that substantial transient pore-water pressure fluctuations, which decrease effective stress and thus the frictional resistance to sliding, are transmitted from the surface to depth in the vertical direction and are well described by a one-dimensional linear diffusion equation (Iverson and Major, 1987; Haneberg, 1991; Reid, 1994; Iverson, 2000; Berti and Simoni, 2010, 2012). According to these

* Corresponding author.
E-mail address: handwerg@uoregon.edu (A.L. Handwerger).

0012-821X/$ – see front matter
http://dx.doi.org/10.1016/j.epsl.2013.06.047

models, the minimum time in which 'strong' pressure change occurs is $T_D = Z^2/D_0$, where Z is landslide depth below the water table and D_0 is characteristic hydraulic diffusivity (Iverson, 2000; Coe, 2012). Calculated values of T_D can serve as a first-order approximation of the pore-water pressure response time. As a result, this simple and frequently used theoretical framework for modeling hydrologically driven changes in landslide velocity suggests that in areas where climate, hillslope angles, and regolith properties are relatively uniform the landslide response time, or the time between the onset of precipitation and landslide acceleration, should scale with the square of landslide depth. Using field-based estimates of hydraulic diffusivity and shear zone depths typical of slow-moving landslides, this model predicts landslide response times to be on the order of days to years. And, in fact, several studies (e.g., Iverson and Major, 1987; Coe et al., 2003; Hilley et al., 2004; Calabro et al., 2010) have documented timescales that are consistent with this range of expected landslide responses.

Iverson and Major's (1987) seminal study of the Minor Creek slide, Northern California, was the first to demonstrate the dominant role of pore-water pressure diffusion in controlling the response of a slow-moving landslide. They found that a simple linear diffusion model could account for the attenuation and phase lag observed in their piezometers, and that landslide acceleration was correlated with a pore-water pressure threshold located at intermediate depths within the slide. Subsequent studies have also found that application of a simple diffusion model can account for the hydrologic response of landslide colluvium (e.g., Haneberg, 1991; Reid, 1994; Berti and Simoni, 2010, 2012). However, no studies have tested how a one-dimensional diffusion model can account for the dynamics of multiple landslides in the same climatic, tectonic, and lithologic area because direct observation of landslide dynamics and hydrologic conditions are often expensive, highly localized, short-lived, and limited to individual landslides in diverse settings.

Simple, homogeneous one-dimensional diffusion models provide a readily accessible, physically-based framework for understanding the hydrologic mechanisms that drive landslide dynamics, but the applicability of these models has not been broadly tested (Berti and Simoni, 2010). One-dimensional diffusion models do not account for discontinuous unsaturated zones, heterogeneous hydraulic properties, surface ponding, or spatial and temporal variations in preferential flow. Landslide hydrology is further complicated by mechanical–hydrologic feedbacks such as shear zone dilation and the development of deformation cracks, which require significant parameterization in order to be incorporated into models (Iverson, 2005; Krzeminska et al., 2013). Deformation cracks are pervasive in clay-rich, slow-moving landslides due to stresses induced by irregular basal topography and changes in deformation (Coe et al., 2009; Krzeminska et al., 2013), yet their effect on landslide behavior is not well understood. These features may have a dual role in affecting landslide stability, in that they facilitate rapid pore pressure transmission to the shear zone as well as increase the drainage efficiency of moving slides (Krzeminska et al., 2013). Currently, there is a lack of spatially explicit data and calibrated models to illustrate how these deformation–hydrology feedbacks influence slow-moving landslides.

Remote sensing techniques have greatly improved our ability to quantify deformation of the earth's surface and provide data with high temporal and spatial resolution. Interferometric synthetic aperture radar (InSAR) can measure mm-scale surface deformation and is a powerful tool for studying a variety of phenomena such as earthquakes (Fialko et al., 2001), volcanoes (Wicks et al., 2002), glaciers (Rignot et al., 2004), land subsidence (Schmidt and Bürgmann, 2003), and landslides (Hilley et al., 2004; Roering et al., 2009; Calabro et al., 2010; Zhao et al., 2012). Previous studies using InSAR in the Eel River catchment have documented multiple active landslides that span an order of magnitude in size and velocity (Roering et al., 2009; Zhao et al., 2012), but these studies did not systematically assess potential linkages between landslide size, depth, and response time.

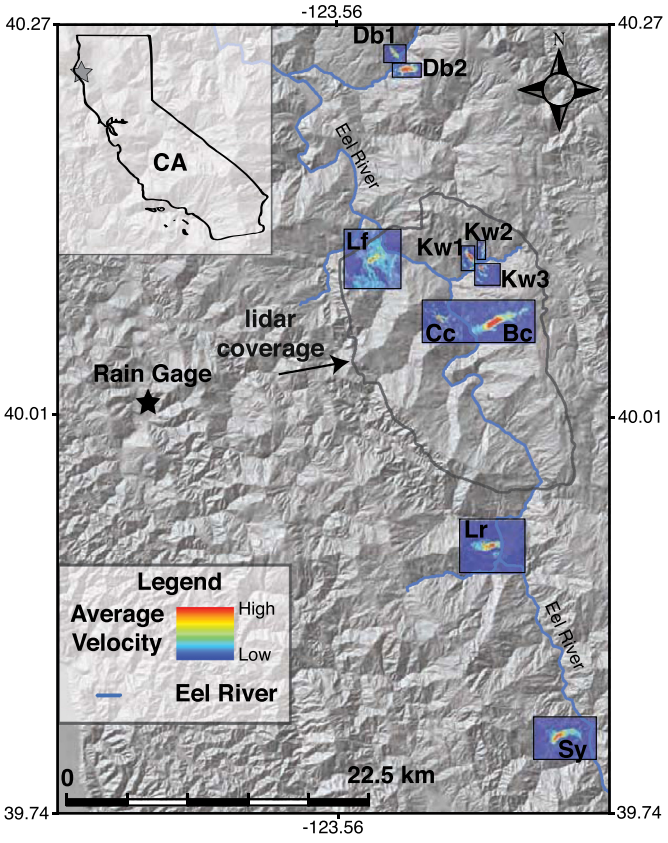

Fig. 1. Eel River catchment, Northern California. Interferograms showing the time-averaged downslope velocity draped over shaded relief. The color scale indicates relative velocity values rather than the actual magnitude values because the velocity range is slightly different for each landslide. Specific landslide velocity magnitudes are reported in Fig. 2. Black star marks the location of the NOAA rain gage. Gray outline indicates lidar coverage. Main stem of the Eel River is outlined in blue. Landslide names are abbreviated as the following: Db1 = Dobbyn Creek 1, Db2 = Dobbyn Creek 2, Lf = Lauffer Road, Kw1 = Kekawaka Creek 1, Kw2 = Kekawaka Creek 2, Kw3 = Kekawaka Creek 3, Cc = Chamise Creek, Bc = Boulder Creek, Lr = Lundblade Ranch, Sy = Simmerly Road. (For interpretation of the references to color in this figure legend, the reader is referred to the web version of this article.)

Here, we use InSAR to construct deformation time series between February 2007 and January 2011 for an inventory of 10 active landslides in the Eel River catchment, Northern California (Fig. 1). Because these slides have similar slope angles and occur within the same tectonic, lithologic, and climatic setting, we are able to analyze the extent to which their collective behavior is consistent with a commonly used one-dimensional diffusion-driven hydrologic model. We explore the relationship between response time and landslide depth derived from field observations, DEMs, and locally-derived scaling relationships. Contrary to model predictions, our data show that slide response to seasonal precipitation is remarkably similar despite a five-fold variation in landslide depth. Our findings challenge and potentially contradict assumptions made in many landslide models that are used for landscape evolution and hazard assessment, and encourage reevaluation of mechanical–hydrologic mechanisms that control landslide dynamics.

2. Slow-moving landslides, Eel River, Northern California

The Eel River catchment is notable for deep-seated, slow-moving slope failures that are induced by highly seasonal pre-

cipitation, weak mélange lithology, and high rates of rock uplift (Kelsey, 1978; Mackey and Roering, 2011). Average annual precipitation is 1.4 m, most of which falls between October and April. The Coast Range is underlain by the Franciscan mélange, a Jurassic–Cretaceous accretionary prism complex that is highly sheared. Our study area lies within the Central Belt of the Franciscan mélange, which is comprised of a mélange matrix surrounding blocks of coherent sandstone, meta-basalt, blueschist, meta-sandstone, and shale (McLaughlin et al., 2000).

The northern Coast Range of California has been tectonically active since the Miocene, largely shaped by the northward migration of the Mendocino Triple Junction (MTJ). Models and geomorphic evidence predict that migration of the MTJ creates a zone of rapid rock uplift, that moves north at 5 cm/yr (Furlong and Govers, 1999; Lock et al., 2006). The resulting uplift gradient influences landscape organization through drainage reversal (fish-hook streams) and river capture (Fig. 1) (Lock et al., 2006). Uplift rates are not well constrained in our field area, but Lock et al. (2006) estimate rates between 0.5 and 1 mm/yr, which is consistent with erosion rates between 0.6 and 1.1 mm/yr derived from suspended sediment data (Wheatcroft and Sommerfield, 2005) and in-situ cosmogenic radionuclides analyzed from stream sediments (Balco et al., in press).

Owing to the persistent activity of slow-moving landslides, the region features relatively low relief, low gradient slopes (average slope $<20°$), and high erosion rates (0.9 mm/yr) (Wheatcroft and Sommerfield, 2005; Booth and Roering, 2011). Landslides in this region, which occupy a relatively small percentage of the total landscape (<10%), contribute a disproportionally large percentage of the regional erosion rate (Swanson and Swanston, 1977; Kelsey, 1980; Kelsey et al., 1995). Mackey and Roering (2011) found that active landslides connected to channels occur in only 6% of our field site and account for >50% of the regionally-averaged denudation rate. Although the role of slow-moving landslides in modulating topographic relief and delivering large boulders to channels has been explored (Booth and Roering, 2011; Booth et al., 2013), less is known about what controls their seasonal dynamics or their potential for catastrophic failure.

We analyzed 10 of these slow-moving landslides, often referred to as earthflows, which exhibit plug flow deformation above narrow shear surfaces (Iverson, 1986; Swanson and Swanston, 1977; Simoni et al., 2013). Each landslide has distinct kinematic zones (e.g., source, transport, and toe) and classical hummocky topography signaling recent movement across much of the terrain (Fig. 2). These failures have areas ranging from 0.16 to 3.1 km^2 and average slope angles of $12 \pm 3°$. From historical air photos, average landslide velocities since the 1960s are 0.2 to 4.2 m/yr and these rates do not appear to vary systematically with landslide size, depth, or average slope (Mackey and Roering, 2011). Analysis of pre-historic landslide rates using meteoric ^{10}Be shows that the Kekawaka 2 landslide has experienced movement for at least 150 years, indicating that these features can sustain perpetual movement for long periods of time (Mackey et al., 2009).

3. Methods

3.1. InSAR

To quantify the seasonal behavior of these 10 landslides, we produced 165 differential interferograms between February 2007 and January 2011 using data acquired by the PALSAR instrument on the ALOS-1 satellite. PALSAR operates with an L-band antenna (23.5 cm) and a 46-day repeat interval. There is a data gap over the summer of 2008 due to large perpendicular baselines, making surface deformation unresolvable during this time. Interferograms were processed using the Repeat Orbit Interferometry Package (ROI PAC) developed at JPL/Caltech (Rosen et al., 2004). Satellite tracks 223 F790 and 224 F790 overlap our field site, and we utilized SAR data from both frames. In contrast to typical landslide studies that require PS-InSAR techniques to quantify deformation (e.g., Hilley et al., 2004), this region is ideal for studies using conventional 2-pass interferometry because the landslides are continuously moving at a rate sufficient to observe deformation in a short time span, yet slow enough to avoid a loss in radar coherence (Roering et al., 2009). We identified active landslides over a range of length scales (<1 to >5 km) by stacking interferograms and then cross checking our InSAR analysis with previously published landslide inventories (Roering et al., 2009; Mackey and Roering, 2011) and high-resolution DEMs (1 m and 10 m grid). To allow for direct comparisons, we back-projected all line-of-sight velocity estimates to the downslope direction of each landslide using their average topographic slope and downslope azimuth inferred from the DEMs and historical air photo-derived displacement vectors (Hilley et al., 2004; Mackey and Roering, 2011).

We employed the method of Schmidt and Bürgmann (2003) to invert 51 small-baseline (<1400 m) interferograms for a smooth time series (Table S1). Our time series processing procedure allowed us to evaluate the translation of any coherent pixel, thus providing complete spatial coverage of each landslide's deformation history (Fig. 2). The nominal sampling interval of our time series is set by the 46-day repeat time interval of the satellite. However, we achieved a temporal sampling as short as ~30 days in certain time periods because we combined SAR data from both overlapping tracks whose data acquisitions are out of phase.

3.2. Landslide depth, soil properties, and response time

We estimated landslide area, slope, and depth with both field and topographic data. For six of the landslides (Boulder Creek, Kekawaka Creek 1, Kekawaka Creek 2, Kekawaka Creek 3, Chamise Creek, and Lauffer Road), we measured landslide depth using lidar (1 m grid) and field observations from longitudinal gullies incised through landslide bodies and from hillslope–channel interfaces where landslide toes are actively truncated by stream erosion. For the four landslides (Simmerly Road, Lundblade Ranch, Dobbyn Creek 1, and Dobbyn Creek 2) that occur outside of the lidar coverage, we calculated depth estimates using a power-law fit to depth–area scaling data derived from 69 landslides in the Eel River catchment mapped from historic aerial photos and lidar (Fig. 3) (Mackey and Roering, 2011). The depth–area relationship is defined by $Z = \alpha A^{\gamma}$, where Z is landslide depth, α is a fit parameter, A is area, and γ is the power-law exponent. Our scaling relationship ($\gamma \sim 0.29$) is in general agreement, but slightly lower than global data sets ($\gamma \sim 0.42$) (Larsen et al., 2010) and a recent earthflow scaling relationship ($\gamma \sim 0.44$) (Simoni et al., 2013). Our landslide depth estimates are not confirmed by borehole data and we likely underestimate the full range of depth values, because our estimated values come from gullies and channels that typically have not fully incised through the landslide mass.

The landslide material is poorly sorted, gravelly clay with occasional large blocks of coherent metasedimentary bedrock (Mackey et al., 2009). Hydraulic investigations at the nearby Minor Creek landslide, which occurs on the same geologic unit as our failures, yields a range of estimates for hydraulic diffusivity spanning 10^{-9} to 10^{-4} m^2/s, but 10^{-6} m^2/s is adopted as the characteristic value (Fig. S1) (Iverson and Major, 1987; Iverson, 2000, 2005). This variability in local (meter-scale) hydraulic conditions likely derives from the significant contrasts in bedrock and regolith properties associated with the Franciscan complex.

To quantify the landslide response time for the 10 landslides, we measured the time lag between the onset of seasonal precipitation and the onset of seasonal acceleration for the WY2008,

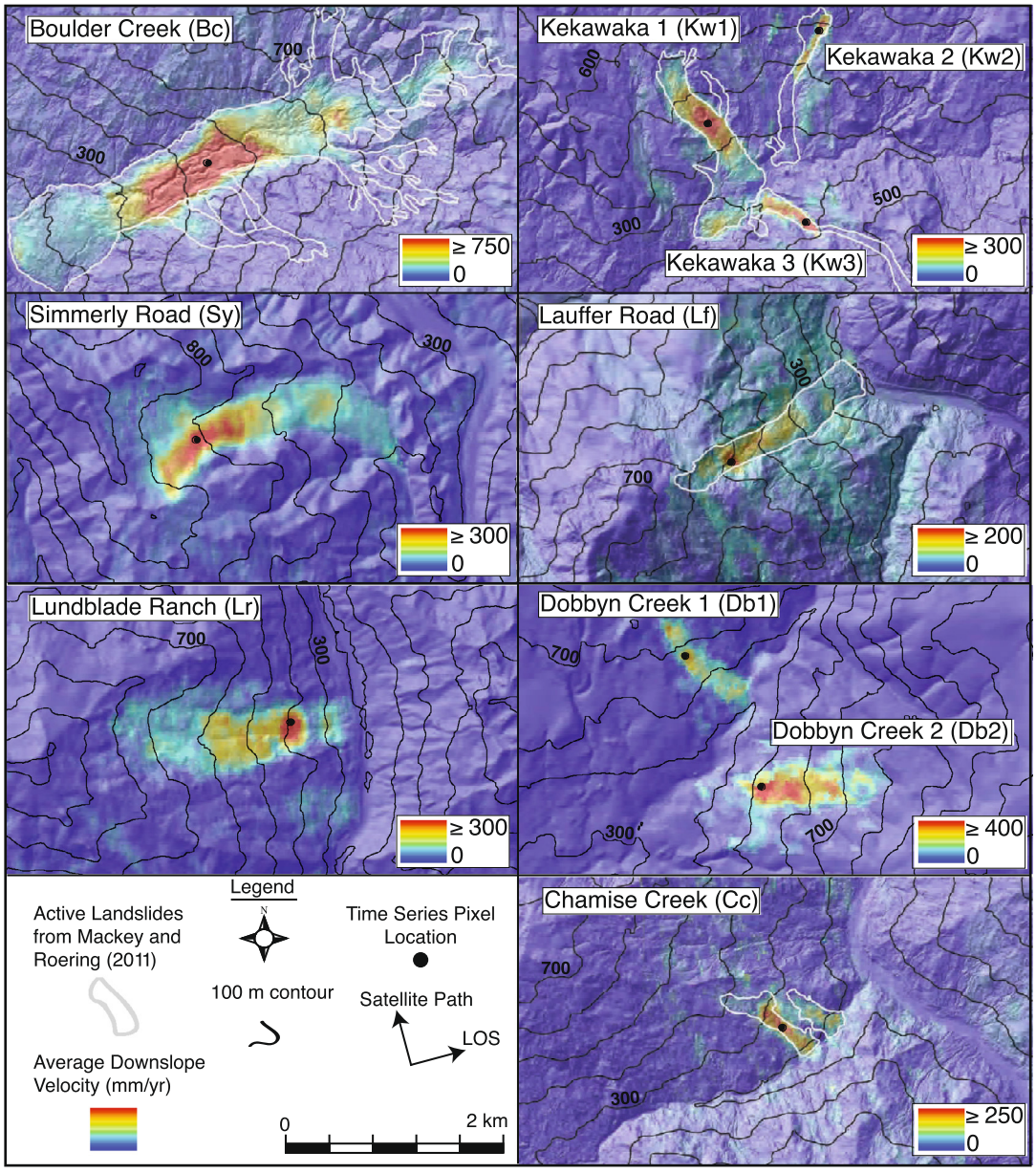

Fig. 2. Time-averaged (2007–2011) downslope velocity draped over shaded relief maps derived from lidar (1 m grid) and 10 m grid. Line-of-sight velocities are projected downslope for each slide using the local slope and azimuth. Color scales were chosen to highlight kinematic zones, not to display the full extent of velocity (i.e. red pixels are $\geqslant$ the maximum listed value). (For interpretation of the references to color in this figure legend, the reader is referred to the web version of this article.)

WY2009, and WY2010. We exclude the WY2010 response time for the Db1 slide (which was 77 days) because that time span is poorly constrained with the InSAR data for that slide; and since Db1's response time is identical to the 9 other slides for WY2008 and WY2009, we are confident the anomalous response is due to an error in the WY2010 data, rather than a valid slide response. Precipitation data was provided by NOAA and was collected at Richardson Grove State Park, Garberville, CA which is ~30 km west of our field area (Fig. 1). We define the onset of seasonal precipitation as the first rainfall event of the water year and the onset of acceleration is delineated as the first SAR acquisition where there is a positive change in velocity after the onset of rainfall.

4. Results

We analyzed 10 landslides that have areas ranging from 0.16 to 3.1 km^2 and estimated average depths that vary from 8 to 40 m (Fig. 2). Each of the landslides exhibits a zone of rapid movement in the central region of the slide, termed the transport zone. Transport zone velocities increased in the wet season and decreased in the dry season for each of the 10 landslides and the landslides exhibited continuous movement throughout the monitoring period (Fig. 4). In agreement with the historic record of landslide velocities in this region from air photos, our InSAR data indicate that the average downslope velocity varied from 0.2 to 1.2 m/yr and these rates show no clear relationship with slide size, average slope, or depth (Table 1). The velocity time series for each slide has a well-defined periodicity of ~1 yr and each landslide responds to seasonal precipitation within 40 days (Fig. 5). This implies that velocity changes, and in particular periods of acceleration following the onset of rainfall, are related to seasonal changes in effective normal stress modulated by transient pore-water pressures. The narrow range of response times belie substantial variation in landslide depth and are much shorter than would be predicted with observed values of diffusivity from the nearby Minor Creek landslide. Our analysis is limited by the ~40 day temporal resolution

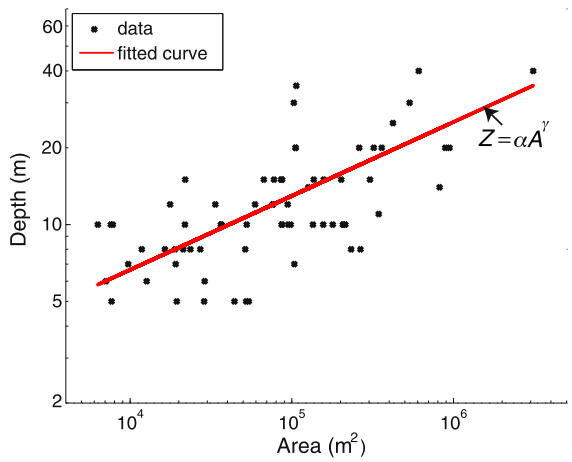

Fig. 3. Depth–area scaling for 69 landslides in the Eel River catchment measured from topographic data using lidar (1 m grid) (Mackey and Roering, 2011). The fitted curve shows a power-function fit with a non-linear least squares regression. The power-function is described by $Z = \alpha A^{\gamma}$, where Z is vertical landslide depth, α is a fit parameter, A is area, and γ is the power-law exponent. We find coefficients (with 95% confidence bound) $\alpha = 0.46$ (0.051, 0.87) and $\gamma = 0.29$ (0.22, 0.36). $R^2 = 0.45$.

of the SAR data set, such that our response times represent maximum estimates; shorter response times elude the resolution of the current InSAR data. Nevertheless, the maximum response times reported here serve as critical constraints to test hydrologic model predictions for each landslide.

5. A simple 1D hydrologic model for landslide response

Given our observations, we seek to reevaluate the applicability of the linear pore pressure diffusion model by using an analytical solution to quantify pressure changes to prescribed perturbations (i.e. rainfall). This analysis yields the magnitude of the pressure change as a function of soil diffusivity, landslide depth, and time. We assume a homogeneous, fully saturated poroelastic medium (e.g., Iverson, 2000). Field investigations of the nearby Minor Creek slide have shown that hydraulic diffusivity is not correlated with depth and that the water table remains within a meter or two of the ground surface year round and approaches the ground surface during the wet season (Iverson and Major, 1987; Iverson, 2000). These observations support the use of the slide thickness as a reasonable approximation of the diffusion length scale and a relatively constant hydraulic diffusivity. However, a more realistic treatment

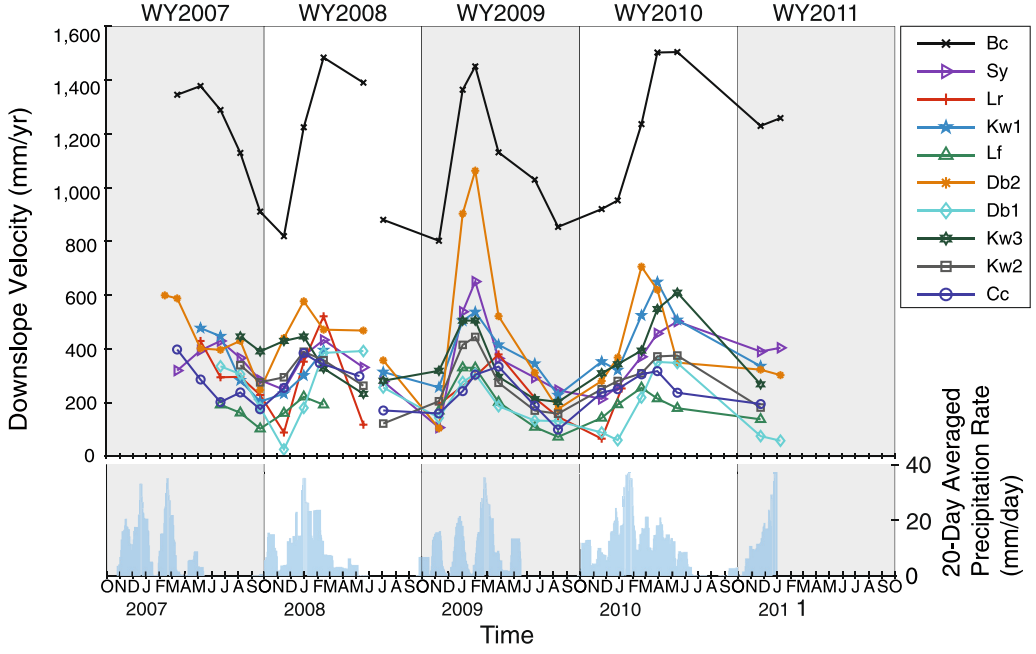

Fig. 4. Downslope velocity time series for the transport zone of each landslide shown with colored lines. The data gap over summer 2008 is due to large perpendicular baselines. Water years (starting Oct 1) are highlighted with white and gray boxes. (For interpretation of the references to color in this figure legend, the reader is referred to the web version of this article.)

Table 1
Landslide metrics. Length is measured as distance from head scarp to toe. Width is calculated using area/length. See text for description of depth estimates. * indicates depth values calculated from our power-law function. Velocity is time averaged over 2007–2011. ^ corresponds to erroneous response time for Db1 (see text for description).

Name	Area (m^2)	Length (m)	Width (m)	Depth (m)	Slope (deg)	Mean downslope velocity (mm/yr)	Response time in days (WY2008, WY2009, WY2010)
Chamise Creek (Cc)	157 549	782	200	15	13	260	36, 37, 40
Kekawaka 2 (Kw2)	208 199	1476	140	10	10	297	36, 37, 40
Kekawaka 3 (Kw3)	232 477	1921	120	8	9	374	36, 37, 40
Dobbyn Creek 1 (Db1)	374 400	1090	340	19*	13	223	36, 37, 77^
Dobbyn Creek 2 (Db2)	506 090	1290	390	21*	15	459	36, 37, 40
Lauffer Road (Lf)	534 981	1906	280	30	14	183	36, 37, 40
Kekawaka 3 (Kw3)	609 348	1818	335	40	10	370	36, 37, 40
Lundblade Ranch (Lr)	1 324 580	2420	550	27*	15	256	36, 37, 40
Simmerly Road (Sy)	1 767 211	2490	710	30*	10	358	36, 37, 40
Boulder Creek (Bc)	3 107 283	4757	653	40	14	1180	36, 37, 40

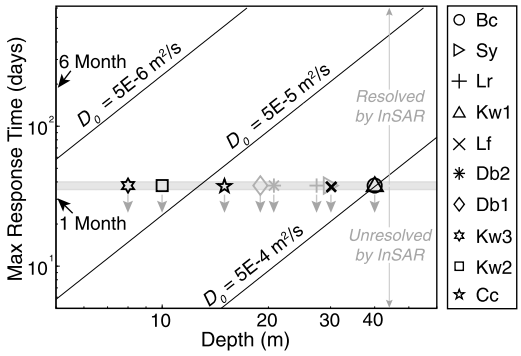

Fig. 5. Maximum landslide response time. Symbols indicate the average maximum landslide response time for individual landslides. Black symbols have depth derived from lidar and gray symbols have depth derived from our scaling relationship. Gray band highlights the range of maximum response times for three water years. Downward pointing arrows emphasize that these are maximum values. Response time values are similar for each slide because the temporal sampling is identical among all of the slides. Solid diagonal lines represent T_D calculated using three diffusivities.

would allow the water table height and the diffusivity to evolve throughout the year as the landslide colluvium wets, dries, and deforms. A one-dimensional pressure diffusion model is given as:

$$\frac{\partial P}{\partial t} = D_0 \frac{\partial^2 P}{\partial Z^2}, \tag{1}$$

where P is the transient pore-water pressure imposed by a change in surface forcing (i.e., precipitation), Z is vertical depth from the water table (assumed to be at the topographic surface) to the shear zone, D_0 is the characteristic hydraulic diffusivity, and t is time. At time $t \leqslant 0$ we assume a background pore-water pressure has developed and then at time $t > 0$ we apply a step change at the surface such that $P(Z = 0, t > 0) = P_0$ and allow it to propagate downwards. Typically, a sinusoidal boundary condition is used at the surface to more accurately represent precipitation events (Iverson and Major, 1987; Haneberg, 1991; Reid, 1994), but we chose to use a step change to clearly distinguish the subsurface response to the discrete onset of rainfall events. Also, rather than employ an arbitrary pressure change at the surface (P_0), we calculate the fraction of surface forcing transmitted to depth (Z) since we do not have observations of the absolute pore pressure. The analytical solution to this problem (Carslaw and Jaeger, 1959) provides the pore-water pressure change as a function of depth and time:

$$\frac{P(Z,t)}{P_0} = erfc\left(\frac{Z}{\sqrt{4D_0 t}}\right), \tag{2}$$

where P/P_0 is the transient pressure as a percentage of the surface forcing. Using (2) we calculated the magnitude of pressure changes that occur within a year (Fig. 6).

Following the onset of precipitation, the diffusion model predicts that the strength of the pore-water pressure wave diffusing through the porous media attenuates with depth (Fig. 6). Thus, landslide thickness and diffusivity are predicted to control the strength and timing of a transient pore-water pressure signal (Iverson and Major, 1987). Studies using a diffusion model with a sinusoidal surface forcing have also found that low frequency pressure changes (i.e. seasonal precipitation) are required to penetrate deep-seated landslides, which has been used to explain why deep-seated, slow-moving landslides respond to seasonal precipitation (Iverson and Major, 1987; Reid, 1994).

6. Potential controls on landslide response

According to diffusion models with values of D_0 typical of those reported for similar soils and our range of slide depths, we expect the landslide response time to vary from days to years (Fig. 5). Instead, we find that landslides of highly varying size and depth respond to rainfall within a narrow range of relatively rapid ($\leqslant$40 days) timescales suggesting several possible explanations: 1) these landslides are sensitive to minor pore-water pressure changes, 2) the diffusivity of these slides is much larger than reported values, and/or 3) a simple, one-dimensional, homogeneous model cannot capture the hydraulic complexity of these slow-moving landslides.

The characteristic diffusion timescale, T_D, is commonly referenced in landslide studies as the minimum time for strong pore-water pressure response and is sometimes used as a first-order approximation of pore-water pressure response (e.g., Coe, 2012), but the exact piezometric response it predicts is rarely stated (Iverson, 2000; Montgomery and Dietrich, 2004). To quantify the pore-water pressure change that corresponds with the diffusion timescale we used Eq. (2) to find

$$\frac{P(Z, T_D)}{P_0} = erfc\left(\frac{1}{2}\right) = 48\%. \tag{3}$$

Eq. (3) shows that the diffusion time scale characterizes the time it takes for 48% of the surface forcing to be felt at depth. We find that T_D is an inappropriate predictor of the timescale for acceleration because these slow-moving slides may respond to subtle pore-water pressure changes that are much less than 48% of the surface forcing and occur well before T_D is reached (Fig. 6).

More importantly, our model results demonstrate that given the typical range of field-derived diffusivity values (Fig. S1), it is unlikely that significant diffusion-driven pressure change occurs in our deepest landslides. For example, if we use the characteristic diffusivity of the Minor Creek landslide (10^{-6} m^2/s), we find <1% diffusive pressure change at depths >7 m within the 40 day response time that can be resolved with our InSAR analysis (Fig. 6D). This suggests that these slides remain close to an acceleration threshold and thus are sensitive to minor pressure changes.

Alternatively, the effective diffusivity that governs slide response could be much higher than values measured in the field. Reported values of diffusivity may underestimate the effective diffusivity that govern slide dynamics because field-based values derive from point measurements that are often selected to avoid heterogeneities (e.g., cracks) (Iverson and Major, 1987; Berti and Simoni, 2010, 2012). Furthermore, because it is common that soil diffusivity ranges over several orders of magnitude within a given landslide (Fig. S1), previous studies have relied on point averaging (e.g., geometric mean), which can lead to a biased characterization of the hydrologic properties of a landslide as related to slide dynamics. For example, Reid (1994) found that diffusion model results accounted for the observed pressure response of the Alani-Paty landslide, Hawaii, using hydrologic parameters derived from the near surface rather than from the entire landslide. Importantly, spatially and temporally continuous measurements may be required to characterize the effective diffusivity of an entire landslide because point measurements or averages of point measurements can easily fail to capture the inherent variability of these parameters.

Preferential flow paths (such as cracks, fissures, and gullies) allow for rapid fluid transmission (up to m/h), are common in actively deforming clay-rich landslides, and are often invoked to explain the rapid response of various hydrologic systems (Beven and Germann, 1982; Berti and Simoni, 2012; Krzeminska et al., 2013). If extensive, vertical-to-subvertical cracks (Fig. S2) connect the near surface to the basal shear zone, they could transmit

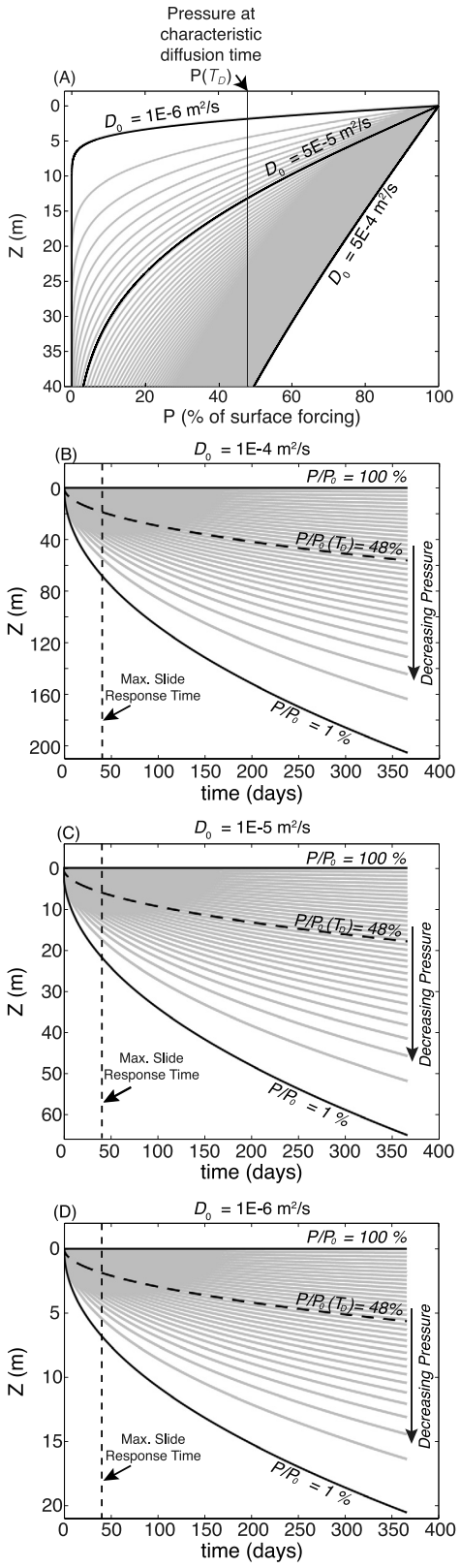

Fig. 6. One-dimensional pore-water pressure diffusion model. (A) Pore-water pressure change that occurs in 40 days (maximum response time) as a function of landslide depth calculated with Eq. (2). Each curved line represents a constant diffusivity. Vertical black line marks the pressure change (48%) that occurs at the characteristic diffusion time scale $P(T_D)$. (B, C, D) Evolution of pore-water pressure over a one-year period using the three common hydraulic diffusivities. (B) $D_0 = 1E{-}4$ m^2/s, (C) $D_0 = 1E{-}5$ m^2/s, (D) $D_0 = 1E{-}6$ m^2/s. Lines are spaced at 3% intervals and represent a constant pressure change. Vertical dashed line marks our observed maximum slide response time.

strong pressure changes much faster than we would predict using field-measured diffusivity values. Iverson and Major (1987) observed the hydrologic response of one such feature; they reported atypical behavior of a >6 m deep well with very low hydraulic diffusivity (10^{-9} m^2/s) that responded almost immediately to rainfall, suggesting proximity to a deep crack. This further exemplifies how point measurements cannot account for heterogeneities that may govern the hydraulic behavior of landslides. The role of preferential pathways in controlling the hydrologic response of soil is not well understood because they are typically overlooked in field studies given that they are difficult to map and extrapolate to depth (Berti and Simoni, 2012).

We also hypothesize that the hydrologic behavior of landslides may be controlled by an effective diffusivity whose value scales with landslide size. This would allow for the effective diffusivity to be larger than can be inferred from field measurements for large slides, while also acting to limit landslide response within a relatively narrow range. This interpretation is inspired by the scale-dependent behavior of longitudinal hydraulic dispersivity, which has been shown to increase as a power-law function of the measurement scale due to an increase in the frequency and/or magnitude of heterogeneities (e.g., high permeability zones) (Schulze-Makuch, 2005).

While the one-dimensional linear diffusion model can describe the hydrologic behavior of homogeneous soil columns (Berti and Simoni, 2010, 2012), our results indicate that the formulation may fail to capture time-dependent hydrologic changes inherent in an evolving mechanical–hydrologic system, such as a landslide. Consistent with our findings, Berti and Simoni (2012) monitored the seasonal pore-water pressure response of landslide-prone terrain and found that while the one-dimensional linear diffusion model could predict shallow (<2 m) transient pressure changes due to individual storms, it could not account for deep (>2 m) seasonal pore-water pressure changes. Current models that predict the hydrologic response of landslides using a linear diffusion model have been invaluable in developing our understanding of these mass movements and can be used to characterize a wide variety of landslide rates and styles (e.g., Iverson, 2000). However, these simplified models do not account for heterogeneities (e.g., spatially and temporally variable diffusivity, mechanical–hydrologic feedbacks) that may control some landslide behavior. Instead a multi-dimensional, heterogeneous diffusion model with mechanical–hydrologic feedbacks may be required to capture the full hydrologic behavior of slow-moving landslides (Krzeminska et al., 2013).

The remarkably consistent seasonal response (i.e. velocity and acceleration) of landslides in our study area suggests that these features may undergo self-organization to maintain a narrow range of basal pore-water pressures, and, thus a narrow range of response times that allows for both long-term motion and seasonal oscillations. This implies that these slides remain close to an acceleration threshold (Iverson and Major, 1987), consistent with the “bathtub model” (Baum and Reid, 2000), a conceptual framework wherein landslides are hydraulically isolated from their surroundings by low permeability shear zones at the base and lateral margins. The hydrologic isolation may allow slides to maintain sufficient pore-water pressure to sustain year-round motion, but also requires that the slides have efficient drainage pathways to prevent catastrophic failure (Iverson, 2005). We hypothesize that the drainage efficiency may evolve each year through shear zone dilation and the connectivity of ephemeral preferential flow paths that help to regulate pore-water pressure (Sidle et al., 2001; Krzeminska et al., 2013). This agrees with observations of internal fractures and pervasive gully networks, which are common to these types of mass movements, and with studies that have quantified mechanical–hydrologic feedbacks such as dilative be-

havior and the development of deformation cracks (Iverson, 2005; Schwab et al., 2008; Schulz et al., 2009; Roering et al., 2009; Krzeminska et al., 2013). Self-regulatory behavior may suggest that these slides are mechanically and hydrologically adjusted to their environment such that they can accommodate daily, seasonal, and multi-year changes in effective stress without failing catastrophically.

7. Conclusions

Our data show that slow-moving landslides in the Eel River catchment exhibit seasonal velocity changes with a periodicity of ~1 yr indicating that they are driven by deep seasonal pore-water pressure changes in basal shear zones. They respond within 40 days following the onset of seasonal rainfall despite significant variations in depth. This observation can be explained in several ways: 1) these slides are sensitive to minor pressure changes in basal shear zones ($\ll$48% of the surface forcing), 2) the effective diffusivity that controls landslide behavior is much larger than those values typically reported (i.e. preferential flow paths) and may scale with landslide size, or 3) a simple, one-dimensional, homogeneous linear diffusion model fails to capture the three-dimensional time-dependent hydrologic changes inherent in an evolving mechanical–hydrologic system, such as a slow-moving landslide. The narrow range in observed response times and persistent movement of the slides is consistent with the idea that these slides maintain a narrow range of pore-water pressure year round and are chronically close to an acceleration threshold such that hydrologic-mechanical feedbacks accommodate seasonal changes in effective stress.

Acknowledgements

We thank Alan Rempel for many insightful discussions about diffusion models. George Hilley and one anonymous reviewer provided helpful reviews. We also thank Richard Iverson, Jon Pelletier, Jeff McDonnell, Mark Reid, Bill Schulz, and Adam Booth for stimulating discussions. We thank Ben Mackey for sharing data. Funding for the research provided by NASA grant number 10-ESI10-0010 and NNX08AF95G. SAR data acquired by JAXA and distributed through ASF.

Appendix A. Supplementary material

Supplementary material related to this article can be found online at http://dx.doi.org/10.1016/j.epsl.2013.06.047.

References

Balco, G., Finnegan, N.J., Gendaszek, A., Stone, J.O.H., Thompson, N., in press. Erosional response to northward-propagating crustal thickening in the coastal ranges of the U.S. Pacific Northwest. Am. J. Sci., http://dx.doi.org/10.2475/11.2013.01.

Baum, R.L., Reid, M.E., 2000. Ground water isolation by low-permeability clays in landslide shear zones. In: Bromhead, E., Dixon, N., Ibsen, M. (Eds.), Landslides in Research, Theory and Practice. Proceedings of the 8th International Symposium on Landslides, vol. 1. Cardiff, Wales. Telford, London, pp. 139–144.

Berti, M., Simoni, A., 2010. Field evidence of pore pressure diffusion in clayey soils prone to landsliding. J. Geophys. Res. 115, F03031.

Berti, M., Simoni, A., 2012. Observation and analysis of near-surface pore-pressure measurements in clay-shales slopes. Hydrol. Process. 26 (14), 2187–2205, http://dx.doi.org/10.1002/hyp.7981 (special issue).

Beven, K., Germann, P., 1982. Macropores and water flow in soils. Water Resour. Res. 18, 1311–1325.

Booth, A.M., Roering, J.J., 2011. A 1-D mechanistic model for the evolution of earthflow-prone hillslopes. J. Geophys. Res. 116 (F4), F04021.

Booth, A.M., Roering, J.J., Rempel, A.W., 2013. Topographic signatures of deep-seated landslides and a general landscape evolution model. J. Geophys. Res. Earth Surf. 118, http://dx.doi.org/10.1002/jgrf.20051.

Bovis, M.J., Jones, P., 1992. Holocene history of earthflow mass movements in south-central British Columbia—The influence of hydroclimatic changes. Can. J. Earth Sci. 29, 1746–1755.

Calabro, M.D., Schmidt, D.A., Roering, J.J., 2010. An examination of seasonal deformation at the Portuguese Bend landslide, southern California, using radar interferometry. J. Geophys. Res. 115, F02020, http://dx.doi.org/10.1029/2009JF001314.

Carslaw, H.S., Jaeger, J.C., 1959. Conduction of Heat in Solids. Oxford University Press, Oxford, England. 510 pp.

Coe, J.A., 2012. Regional moisture balance control of landslide motion: Implications for landslide forecasting in a changing climate. Geology 40, 323–326.

Coe, J.A., Ellis, W.L., Godt, J.W., Savage, W.Z., Savage, J.E., Michael, J.A., Kibler, J.D., Powers, P.S., Lidke, D.J., Debray, S., 2003. Seasonal movement of the Slumgullion landslide determined from global positioning system surveys and field instrumentation, July 1998–March 2002. Eng. Geol. 68, 67–101, http://dx.doi.org/10.1016/S0013-7952(02)00199-0.

Coe, J.A., McKenna, J.P., Godt, J.W., Baum, R.L., 2009. Basal-topographic control on stationary ponds on a continuously moving landslide. Earth Surf. Process. Landf. 34, 264–279.

Fialko, Y., Simmons, M., Agnew, D., 2001. The complete (3-D) surface displacement field in the epicentral area of the 1999 Mw7.1 Hector Mine earthquake, California, from space geodetic observations. Geophys. Res. Lett. 28 (17), 3063–3066.

Furlong, K.P., Govers, R., 1999. Ephemeral crustal thickening at a triple junction: The Mendocino crustal conveyor. Geology 27 (20), 127–130.

Haneberg, W.C., 1991. Pore pressure diffusion and the hydrologic response of nearly saturated, thin landslide deposits to rainfall. J. Geol. 99, 886–892.

Hilley, G.E., Bürgmann, R., Ferretti, A., Novali, F., Rocca, F., 2004. Dynamics of slow-moving landslides from permanent scatterer analysis. Science 304, 1952–1955.

Iverson, R.M., 1986. Unsteady, nonuniform landslide motion: 1. Theoretical dynamics and the steady datum state. J. Geol. 94, 1–15.

Iverson, R.M., 2000. Landslide triggering by rain infiltration. Water Resour. Res. 36, 1897–1910, http://dx.doi.org/10.1029/2000WR900090.

Iverson, R.M., 2005. Regulation of landslide motion by dilatancy and pore-pressure feedback. J. Geophys. Res. 110, F02015.

Iverson, R.M., Major, J.J., 1987. Rainfall, ground-water flow, and seasonal movement at Minor Creek landslide, northwestern California: Physical interpretation of empirical relations. Geol. Soc. Am. Bull. 99, 579–594, http://dx.doi.org/10.1130/0016-7606(1987)99<579:RGFASM>2.0.CO;2.

Iverson, R.M., Reid, M.E., Iverson, N.R., LaHusen, R.G., Logan, M., Mann, J.E., Brien, D.L., 2000. Acute sensitivity of landslide rates to initial soil porosity. Science 290, 513–516.

Kelsey, H.M., 1978. Earthflows in Franciscan mélange, Van Duzen River basin, California. Geology 6, 361–364.

Kelsey, H.M., 1980. A sediment budget and an analysis of geomorphic process in the Van Duzen River Basin, north coastal California, 1941–1975—Summary. Geol. Soc. Am. Bull. 91 (4), 190–195.

Kelsey, H.M., Coghlan, M., Pitlick, J., Best, B., 1995. Geomorphic analysis of streamside landslides in the Redwood Creek Basin, northwestern California. In: Nolan, K.M., Kelsey, H.M., Marron, D.C. (Eds.), Geomorphic Processes and Aquatic Habitat in the Redwood Creek Basin, Northwestern California. In: U.S. Geological Survey Professional Papers, vol. 1454, pp. J1–J12.

Krzeminska, D.M., Bogaard, T.A., Malet, J.-P., van Beek, L.P.H., 2013. A model of hydrological and mechanical feedbacks of preferential fissure flow in a slow-moving landslide. Hydrol. Earth Syst. Sci. 17, 947–959.

Larsen, I.J., Montgomery, D.M., Korup, O., 2010. Landslide erosion controlled by hillslope material. Nat. Geosci. 3, 247–251.

Lock, J., Kelsey, H., Furlong, K., Woolace, A., 2006. Late Neogene and quaternary landscape evolution of the northern California Coast Ranges: Evidence for Mendocino triple junction tectonics. Geol. Soc. Am. Bull. 118, 1232–1246.

Mackey, B.H., Roering, J.J., 2011. Sediment yield, spatial characteristics, and the long-term evolution of active earthflows determined from airborne LiDAR and historical aerial photographs, Eel River, California. Geol. Soc. Am. Bull. 123, 1560–1576, http://dx.doi.org/10.1130/B30306.1.

Mackey, B.H., Roering, J.J., McKean, J.A., 2009. Long-term kinematics and sediment flux of an active earthflow, Eel River, California. Geology 37, 803–806.

McLaughlin, R.J., Ellen, S.D., Blake Jr., M.C., Jayko, A.S., Irwin, W.P., Aalto, K.R., Carver, G.A., Clarke Jr., S.H., 2000. Geology of the Cape Mendocino, Eureka, Garberville, and southwestern part of the Hayfork 30 × 60 minute quadrangles and adjacent offshore area, Northern California. U.S. Geological Survey Miscellaneous Field Studies Map MF-2336, 1:100 000 scale.

Montgomery, D.R., Dietrich, W.E., 2004. Reply to comment by Richard M. Iverson on "Piezometric response in shallow bedrock at CB1: Implications for runoff generation and landsliding". Water Resour. Res. 40, W03802.

Moore, P.L., Iverson, N.R., 2002. Slow episodic shear of granular materials regulated by dilatant strengthening. Geology 30, 843–846.

Petley, D.N., Bulmer, M.H., Murphy, W., 2002. Patterns of movement in rotational and translational landslides. Geology 30, 719–722.

Reid, M.E., 1994. A pore-pressure diffusion model for estimating landslide-inducing rainfall. J. Geol. 102, 709–717.

Rignot, E., Casassa, G., Gogineni, P., Krabill, W., Rivera, A., Thomas, R., 2004. Accelerated ice discharge from the Antarctic Peninsula following the col-

lapse of Larson B ice shelf. Geophys. Res. Lett. 31, L18401, http://dx.doi.org/10.1029/2004GL020697.

Roering, J.J., Stimely, L.L., Mackey, B.H., Schmidt, D.A., 2009. Using DInSAR, airborne LiDAR, and archival air photos to quantify landsliding and sediment transport. Geophys. Res. Lett. 36, L040374.

Rosen, P.A., Henley, S., Peltzer, G., Simons, M., 2004. Updated repeat orbit interferometry package released. Eos Trans. AGU 85 (5), 47, http://dx.doi.org/10.1029/2004EO050004.

Rutter, E.H., Green, S., 2011. Quantifying creep behaviour of clay-bearing rocks below the critical stress state for rapid failure: Mam Tor landslide, Derbyshire, England. J. Geol. Soc. 168, 359–372.

Scheingross, J.S., Minchew, B.M., Mackey, B.H., Simons, M., Lamb, M.P., Hensley, S., 2013. Fault-zone controls on the spatial distribution of slow-moving landslides. Geol. Soc. Am. Bull. 125, 473–489, http://dx.doi.org/10.1130/B30719.1.

Schmidt, D.A., Bürgmann, R., 2003. Time-dependent land uplift and subsidence in the Santa Clara valley, California, from a large interferometric synthetic aperture radar data set. J. Geophys. Res. 108, B002267.

Schulz, W.H., McKenna, J.P., Kibler, J.D., Biavati, G., 2009. Relations between hydrology and velocity of a continuously moving landslide—Evidence of pore-pressure feedback regulating landslide motion? Landslides 6, 181–190, http://dx.doi.org/10.1007/s10346-009-0157-4.

Schulze-Makuch, D., 2005. Longitudinal dispersivity data and implications for scaling Behavior. Ground Water 43, 443–456.

Schwab, M., Rieke-Zapp, D., Schneider, H., Liniger, M., Schlunegger, F., 2008. Landsliding and sediment flux in the Central Swiss Alps: A photogrammetric study of the Schimbrig landslide, Entlebuch. Geomorphology 97 (3), 392–406.

Sidle, R.C., Noguchi, S., Tsuboyama, Y., Laursen, K., 2001. A conceptual model of preferential flow systems in forested hillslopes: evidence of self-organization. Hydrol. Process. 15, 1675–1692.

Simoni, A., Ponza, A., Picotti, V., Berti, M., Dinelli, E., 2013. Earthflow sediment production and Holocene sediment record in a large Apennines catchment. Geomorphology 188, 42–53.

Swanson, F.J., Swanston, D.N., 1977. Complex mass movement terrains in the western Cascade Range, Oregon. Rev. Eng. Geol. 3, 113–124.

Terzaghi, K., 1950. Mechanism of landslides. In: Engineering Geology (Berkey) Volume. Geol. Soc. Am., pp. 83–123.

Wheatcroft, R.A., Sommerfield, C.K., 2005. River sediment flux and shelf sediment accumulation rates on the Pacific Northwest margin. Cont. Shelf Res. 25, 311–332.

Wicks, C.W., Dzurisin, D., Ingebritsen, S., Thatcher, W., Lu, Z., Iverson, J., 2002. Magmatic activity beneath the quiescent Three Sisters volcanic center, central Oregon Cascade Range, USA. Geophys. Res. Lett. 29 (7), http://dx.doi.org/10.1029/2001GL014205.

Zhao, C., Lu, Z., Zhang, Q., de la Fuente, J., 2012. Large-area landslide detection and monitoring with ALOS/PALSAR imagery data over Northern California and Southern Oregon, USA. Remote Sens. Environ. 124, 348–359.